2.5 Ring to Main Linac Section

Andrea Latina, CERN, CH 1211 Geneva 23, Switzerland
Mail to: mailto:andrea.latina@cern.ch

2.5.1 Introduction

Primarily the "Ring to Main Linac" (RTML) of CLIC has the function of transporting the beam from the damping ring extraction to the main linac entrance. Two RTML sections are present in CLIC: one for the electron side and one for the positron side of the machine. Each section involves more than 25 km of beamlines and includes specific subsystems to accomplish various tasks and beam manipulations:

1. Matching the requirements of the CLIC geometric layout, transporting the beam from the damping ring extraction located in the center of the site to the entrance of the main linacs located at the two opposite ends of the site; this involves horizontal and vertical doglegs, a turnaround loop, and a long transfer line;
2. Accelerating the beam from 2.86 to 9 GeV while compressing the bunches longitudinally from 1.6 mm to 44 μm bunch length;
3. Controlling the spin of the electrons to achieve any orientation.

These three tasks must be accomplished while: preserving the nanometer transverse emittances, protecting the linac from errant beams and halo particles, measuring the relevant beam parameters for on-line diagnostics.
The presented RTML design is suitable also for different stages of CLIC, because the beam parameters at damping ring extraction and at linac entrance are similar at the different stages. The most significant change regards the long transfer lines, which at 500 GeV are shorter to match the shorter linac length. A detailed description of the entire system can be found in [1].

2.5.2 System Description

The two RTMLs for electrons and positrons have each a total length of approximately 27 km. Their layouts are similar, but there are small differences due to geometric constraints and to the fact that positron polarization is not included in the CLIC baseline. The layout of the RTML is shown in Fig. 1. Not visible in the figure is that the RTML must also descend below the ground level, since the damping rings are located on the site surface whereas the main linac is 100 m underground.

Table 1: Main beam parameters at the entrance and at the exit of the RTML.

Parameter	*Entrance*	*Exit*	*Unit*
Energy	2.86	9	GeV
RMS bunch length	1600	44	μm
RMS energy spread	0.13%	<1.7%	
Normalized horizontal emittance	500	<600	nm
Normalized vertical emittance	5	<10	nm

The RTML is composed by several distinct subsystems, which will be described in the following sections, connected by short matching sections. The beam parameters at

the entrance and at the exit of the RTML are the same for both electrons and positrons, and are listed in Table 1.

2.5.2.1 *Electron Spin Rotator*

A spin rotator is located at the start of the electron RTML. Its design consists in two pairs of solenoid magnets, separated by a bending arc. Between each solenoid pair, a reflector beam line with transfer matrix (I 0 ; 0 –I) is used to cancel the couplings induced by the solenoids. Each solenoid pair can be set independently, allowing a spin rotation from 0 to 90 degrees. The arc in between the solenoid pairs bends the beam by an angle of 13.9 degrees, which corresponds to a spin rotation by 90 degrees. The combination of the two tuneable solenoid pairs with the bending arc allows the achievement of any arbitrary spin orientation. The momentum compaction factor of the arc is small, only 5.9 cm, which limits the bunch lengthening to 2 μm taking into account the small energy spread of the beam, 0.13%. [2,3].

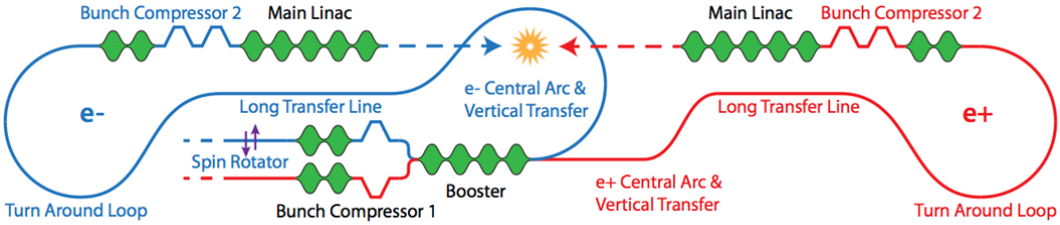

Figure 1: A scheme of the CLIC RTML.

2.5.2.2 *Bunch Compressors and Booster Linac*

To control the longitudinal phase space, both electron and positron lines are equipped with two bunch compressors and a booster linac. Bunch compressor 1 is located at the beginning of the RTML, where the beam has energy 2.86 GeV; bunch compressor 2 is located right before the main linac entrance, at 9 GeV. The beam energy is brought from 2.86 to 9 GeV in the booster linac, right before the central arc and the long transfer line.

The first stage of bunch compression (BC1) compresses the initially 1.6 mm long bunches to a length of 300 μm. Its RF section consists of twenty 2 GHz cavities embedded in a FODO lattice identical to that for the booster linac. Each cavity has a length of 1.5 m and an average gradient of 13.3 MV/m. The beam passes through the cavities at a phase of 90 degrees off-crest, i.e. at zero crossing, so there is in average there is no acceleration but this leads to an almost linear energy which is required to compress the bunches to 300 μm in the chicane that follows, which has R_{56} =-14.5 m.

The setup of the bunch compressors is the result of an optimization process that takes into account effects like coherent synchrotron radiation (CSR) and incoherent synchrotron radiation (ISR) [4], the energy acceptance of the downstream arcs, beam phase stability and RF properties [5,6].

The booster linac accelerates the beam to the main linac injection energy of 9 GeV. The same linac is shared between electrons and positrons. The two incoming bunch trains are shifted in time by 1100 ns, based on RF constraints. The booster linac has the same type of 2 GHz cavities as BC1. There are a total of 276 cavities at an average

gradient of 14.9 MV/m. They are embedded into a FODO lattice with 8 cavities per cell with an average beta function of 16 m. The total length of the booster linac is 538 m.

The second bunch compressor (BC2) compresses the bunch length to 44 μm. It contains an RF section with 78 12 GHz cavities which are 0.23 m long and run 90 degrees off-crest with an average gradient of 94 MV/m. The impact of longitudinal short-range wakefields, that tends to lower the energy chirp, is taken into account. To ensure that the short-range wakefields do not degrade the beam quality, the BC2 lattice is the same as the start of the main linac. To limit the impact of ISR, the required R_{56} is obtained using two chicanes, with R_{56} equal to -1.38 and -0.60 cm respectively. Full bunch compression is achieved, as it increases stability in the main linac.

2.5.2.1 *Central Arc and Turnaround Loop*

The central arcs transport the beams from the booster linac horizontally, and descend 100 m underground to the main linac tunnels. The electrons are bent by 180 degrees in the central arc, and sent toward the linac entrance. The positron beam exits the booster pointing already toward the right direction, thus the central arc is just a dog-leg with the vertical transfer to reach the main linac tunnel. Both lines can compensate for the timing offset between electrons and positrons and implement a feed forward system to counteract incoming transverse beam jitter. Given the shorter length of the positron line, with respect to the electron one, the feed forward correction scheme is more challenging for positrons than for electrons.

The electron central arc has an average radius of 305 m, featuring the same cell design as the turnaround loops. Each cell is 31.9 m long and produces a 6 degrees bend, with five dipoles, seven quadrupoles and four sextupoles. The phase advance is 432 in the horizontal plane and 144 in the vertical plane. It's achromatic, almost isochronous, and optimized for acceptable emittance growth due to incoherent synchrotron radiation (ISR) [1]. Figure 2 shows the optics functions in a single cell, including the dispersion R_{16} and the R_{56}. The central arc is composed by 30 of such cells.

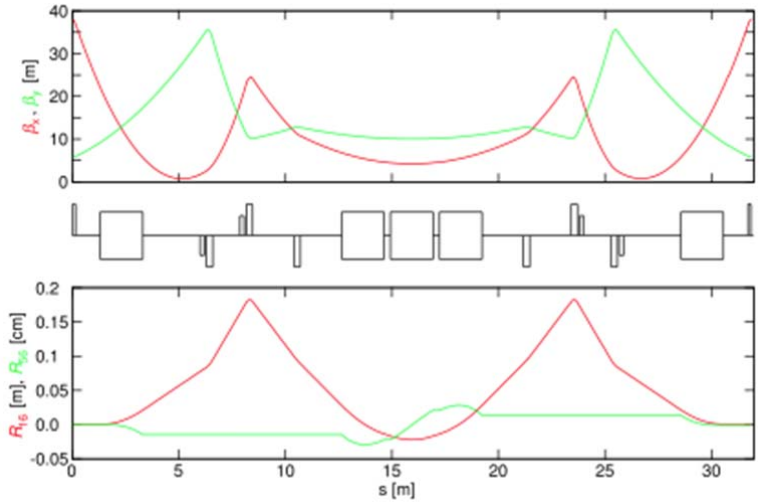

Figure 2: Beta functions (top), dispersion and momentum compaction (bottom) in an arc cell.

The two turnaround loops direct the outgoing beams towards the interaction point (IP). The beams are bent by 180 degrees and the resulting horizontal offsets are

corrected by dog-legs. The choice of two 60 degrees arcs per dog-leg is a compromise between limiting ISR and lattice length. The arcs of each dog-leg are connected by a periodic lattice 354 m long. The average radius of the arcs is again 305 m and the total loop length is 1944 m. Both turnaround loops contain 50 arc cells.

2.5.2.2 *Long Transfer Line*

Long 21 km transfer lines transport the beams from the central region, where the booster is located, to the far ends of the main linac tunnel. They consist of a FODO lattice with very weak quadrupoles, $k_1 = 0.0097$ m^{-2}, resulting in a cell length of 438 m and an average beta function of 620 m. The phase advance is 45 degrees. A beam pipe radius of 6 cm reduces resistive wall wakefields that could cause multi-bunch instability [7,8]. To suppress the fast beam-ion instability, the vacuum must be below 10^{-10} mbar [8]. Studies of emittance preservation showed that a quadrupole pre-alignment of 100 μm is adequate even when only correcting with one-to-one steering [9]. On the other hand, studies show that there are very tight tolerances on the allowed dynamic variation of stray magnetic fields. Periodic stray fields with a wavelength equal to the betatron wavelength must be below 10 nT with a variation of 0.1 nT [5,10].

2.5.3 **Emittance Preservation**

The lengths of the RTML sections are approximately 27 km each. Limiting the emittance growth over this distance is one of the major challenges for the design. Three emittance budgets have been set for the RTML, as they are summarized in Tab. 2: design, static, and dynamic. It is required that the machine remains below the static emittance growth budgets with a probability of 90%. The design budget prescribes that the design emittance growth intrinsic to the design stays below 60 nm in horizontal axis, and below 1 nm in the vertical axis. The static and dynamic budgets account for the impact of the static misalignment of the elements, and for dynamic imperfections such as ground motion, vibrations and stray fields.

Table 2: CLIC RTML emittance growth budgets in nm.

	Design	***Static***	***Dynamic***	***Total***
Horizontal emittance	60	20	20	100
Vertical emittance	1	2	2	5

The effect causing the largest emittance growth even in a perfect system is the emission of incoherent synchrotron radiation (ISR) in the bending magnets. ISR absorbs about 40 nm of the horizontal emittance budget for the electron beam, and about 25 nm for the positron beam (that does not require a central arc). In the vertical plane, where only weak arcs are required in the transfer tunnels, the ISR emittance growth is less than 1 nm. The second largest contribution to the emittance growth is the emission of coherent synchrotron radiation (CSR) in the bunch compressor chicanes. CSR absorbs 20 nm of the total budget in the horizontal plane. The CSR effect can be mitigated shielding the conducting walls of the vacuum chamber. It has been calculated that, for the shielding to be effective, the vertical aperture must be smaller than about 2 cm. The baseline design fulfills the design emittance growth budget, as it is shown in Fig. 3 for the horizontal axis.

2.5.3.1 *Static Misalignments and Beam-based Alignment*

The misalignment of the accelerator components with respect to a reference line, due to imperfect pre-alignment, impacts the beam quality by inducing emittance growth via dispersive and chromatic effects in the quadrupoles, and via short- and long- range wakefields in the accelerating structures. Given the very small vertical emittance, and the tight bu

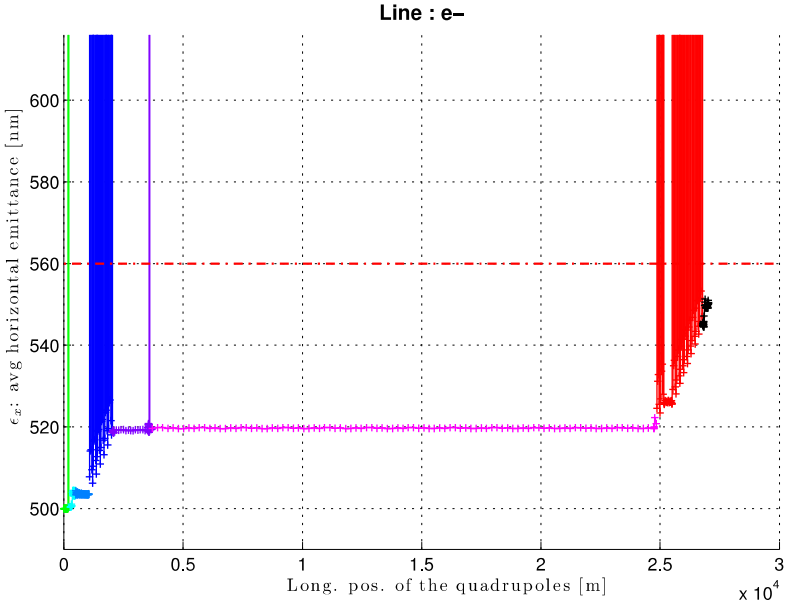

Figure 3: Emittance growth induced by wakefields and synchrotron radiation in the electron RTML.

The effect of static misaligned components is reduced by beam-based alignment (BBA) techniques. Standard BBA algorithms, such as 1:1 correction and dispersion-free steering, have been tested in each subsystem of the RTML, and pre-alignment tolerances have been drawn. Table 3 summarizes the expected RMS pre-alignments that induce 1 nm emittance growth in the vertical axis. Some of the subsystems, like the central arc, the turnaround loop and the bunch compressor 2, are quite tight. Studies are being carried out to relax these tolerances: for instance, finely tuned BBA algorithms, and the usage of more precise beam position monitors (BPMs), already proved to be useful. For example, the simulations have been performed assuming 1 μm BPM resolution: testing a resolution of 0.1 μm has relaxed these tolerances by a factor 1.3 [11].

2.5.4 **Dynamic Imperfections**

Dynamic imperfections such as ground motion, vibrations, stray fields, jitter in the accelerator components and incoming beam jitter can induce emittance growth and ultimately luminosity loss. The RTML, where the bunches travel for more than 25 km and undergo significant transformation of their longitudinal profile through acceleration and bunch length compression, is one of the most critical systems both in the transverse and the longitudinal planes.

Table 3: Average tolerance in μm obtained after applying 1:1 and DFS correction. In brackets the value corresponding to the 90-th percentile curve.

Subsystem	*1:1*	*DFS*
Spin Rotator & Bunch compressor 1	17 (11)	55 (24)
Booster	29 (19)	45 (23)
Central arc	7 (5)	14 (7
Long transfer line	153 (88)	280 (150)
Turnaround loop	6 (4)	9 (5)
Bunch compressor 2	1.4 (0.8)	3.5 (2)

2.5.4.1 *Phase Stability*

In the bunch compressors the longitudinal phase space is rotated to achieve compression. This means that energy and phase errors are coupled, with phase errors turning into energy errors and vice versa. This casts stringent requirements on the gradient and phase stability of the RF system of bunch compressor 1 and 2, and of the booster linac [6].

The requirement that luminosity loss due to phase errors must be less than 2% imposes the relative phasing of Main Beam and Drive Beam to be better than 0.2 degrees (at 12 GHz) for coherent errors along the Drive Beam sections, and better than 0.8 degrees (at 12 GHz) for errors incoherent along the Drive Beam sections. The relative phasing of electrons and positrons at the IP has to be better than 0.4 degrees (at 12 GHz). These constraints facilitate the specification of the allowed beam phase errors at ML entrance for the two different phase references under consideration. In case of external phase references (EPR) the beam phase stability in front of the ML has to be better than < 0.2 degrees (at 12 GHz), since any phase error of the Main Beam will remain unchanged along the entire ML and will thus be coherent in all drive-beam sections. In case the outgoing beams are used as reference (OBR) two values need to be specified: since the Main Beam including a possible phase error is used as phase reference for the RF of the second bunch compressor and the Drive Beam the relative phasing will always be correct. Hence, the allowed beam phase error is limited to < 0.4 degrees (at 12 GHz) by the relative phasing of electrons and positrons at the IP. On the other hand, any phase error imposed on the Main Beam behind the phase measurement has to stay below < 0.2 degrees (at 12 GHz) to avoid spoiling the relative phasing of Main Beam and Drive Beam [1]. A feed forward correction scheme to ensure phase stability is being designed based on the experience gained in studies such as [12,13].

2.5.4.2 *Transverse Stability*

Detailed studies of the impact of ground motion, vibrations, stray fields, jitter in the accelerator components on transverse emittance growth and orbit stability are in progress.

To reduce the emittance growth due to incoming beam jitter from the damping ring extraction kicker, a feed forward system is presented in [14]. It consists of two feed forward systems situated across the central arcs (CAs) and turnaround loops (TALs). A beam position monitoring region will be situated upstream of each arc section and a kicker region situated downstream; the feed forward signals will cut across the arc, allowing it to travel a shorter path and arrive earlier than the beam. The beam position

monitor region will be used to determine the position and angle trajectories in both the horizontal and vertical planes. This information is then used to determine the kicker corrections required by the feed forward electronics and the kickers are fired accordingly. The horizontal and vertical feed forward systems are completely independent of each other and use different BPMs and kickers. This is to simplify each feed forward system to a 2-dimensional problem rather than a 4-dimensional one; which reduces the required computing power of each feed forward system. Details on the required electronics and kicker specifications for this system can be found in [14].

Detailed simulations to compare the emittance growth with and without feed forward correction are shown in Fig. 4. In the figure it is visible that the amplitude of the beam jitter at the end of the RTML is reduced by a factor ≈ 10 in the horizontal plane and ≈ 6 in the vertical plane when the feed forward corrections are applied.

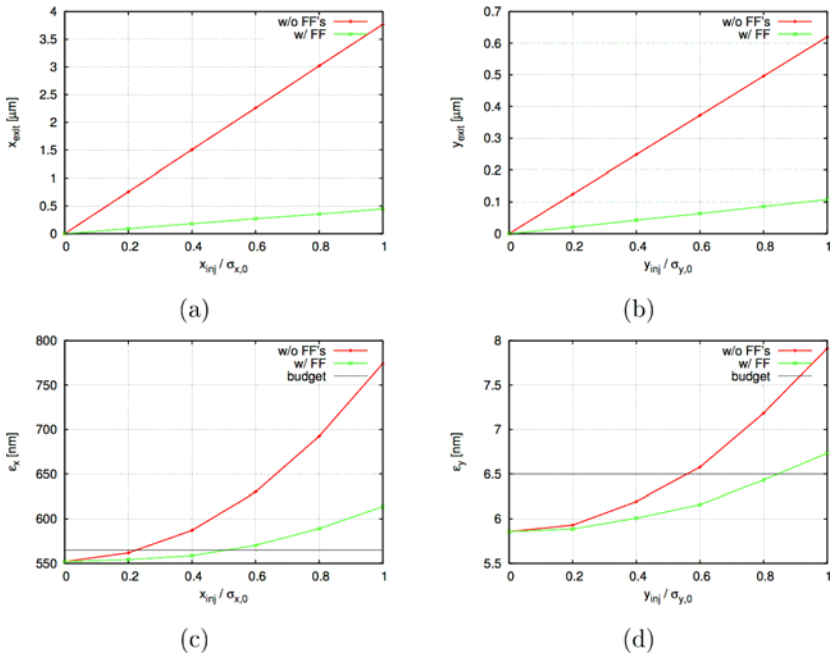

Figure 4: Plots of the orbit jitter (a, b) and normalised emittance (c, d) at the exit of the RTML versus orbit jitter at the entrance of the RTML in the horizontal and vertical planes respectively.

2.5.5 References

1. *CLIC Conceptual Design report*, CERN-2012-007 (CERN, 2012).
2. Emma, P. A spin rotator system for the NLC, NLC-Note-7 (SLAC, Stanford, CA, USA, 1994).
3. Latina, A., Solyak, N. & Schulte, D. in Proc. 1st Int. Particle Accelerator Conf., 23-28 May 2010, Kyoto, Japan (2010), 4608–4610. <http://accelconf.web.cern.ch/accelconf/IPAC10/papers/thpe040.pdf>.
4. Stulle, F., Adelmann, A. & Pedrozzi, M. Conceptual design of bunch compressors and turn around loops for a multi-TeV linear collider EUROTeV-Report-2008-025 (CERN, 2008). <http://www.eurotev.org/sites/site_eurotev/content/e328/e329/e1082/e1500/EUROTeV-Report-2008-025.pdf>.
5. Stulle, F., Schulte, D., Snuverink, J., Latina, A. & Molloy, S. in Proc. XXV Linear

Accelerator Conf., 12-17 September 2010, Tsukuba, Japan (2010), 88–90. <http://accelconf.web. cern.ch/accelconf/LINAC2010/papers/mop019.pdf>.
6. Stulle, F. *Beam phase and energy tolerances in the CLIC RTML* CERN-OPEN-2011-048. CLIC- Note-874 (CERN, 2011). <http://cdsweb.cern.ch/record/1406047/files/ CERN-OPEN-2011-048.pdf >.
7. Jeanneret, J. B. & Braun, H.-H. in *Proc. 11th European Particle Accelerator Conf., 23-27 June 2008, Genoa, Italy* (2008), 3014–3016. <http://accelconf.web.cern.ch/accelconf/ e08/papers/thpc017.pdf>.
8. Jeanneret, J. B. *et al.* in *Proc. 11th European Particle Accelerator Conf., 23-27 June 2008, Genoa, Italy* (2008), 3017–3019. <http://accelconf.web.cern.ch/accelconf/e08/ papers/thpc018.pdf>.
9. Stulle, F., Schulte, D., Snuverink, J., Latina, A. & Molloy, S. in *Proc. 1st Int. Particle Accelerator Conf., 23-28 May 2010, Kyoto, Japan* (2010), 3013–3015. <http://accelconf.web. cern.ch/accelconf/IPAC10/papers/wepec054.pdf>.
10. Snuverink, J. *et al.* in *Proc. 1st Int. Particle Accelerator Conf., 23-28 May 2010, Kyoto, Japan* (2010), 3398–3400. <http://accelconf.web.cern.ch/accelconf/IPAC10/ papers/wepe023.pdf>.
11. Lienart, T. *Study of pre-alignment tolerances in the RTML* CERN-OPEN-2012-014. CLIC-Note-943. (CERN, 2012). <https://cds.cern.ch/record/1452626/files/CERN-OPEN-2012-014.pdf>
12. Gerbershagen, A. *CLIC Drive Beam Phase Stabilisation*, Phd Thesis (University of Oxford, 2013)
13. Skowronski, P. et al. *Design of Phase Feed Forward System in CTF3 and Performance of Fast Beam Phase Monitors* CERN-ACC-2013-0092 (CERN, 2013) <https://cds.cern.ch/record/1575566/files/CERN-ACC-2013-0092.pdf>
14. Apsimon, R. and Latina, A. *Proposed Feed Forward Correction for the CLIC Ring-To-Main-Linac Transfer Lines* CLIC Note *to be published*

2.6 RF Design of the CLIC Main Linac Accelerating Structure

Alexej Grudiev, CERN, CH 1211 Geneva 23, Switzerland
Mail to: Alexej.Grudiev@cern.ch

2.6.1 Introduction

The parameters of the CLIC main linac accelerating structure have been obtained based on an optimization which includes an improved understanding of high-gradient limits, wakefields related beam dynamics constrains and integrates the performance and cost of CLIC at 3 TeV (see more details in [1,2]). Furthermore, compact couplers have been developed and HOM damping loads have been designed. The rf design has also been made consistent with details of the manufacturing procedure, which is based on bonded asymmetrical disks, and with requirements coming from integration of the accelerating structure in the two-beam module.